13th International Conference on
Structural Health Monitoring of Intelligent Infrastructure
DOI: 10.3217/978-3-99161-057-1-172

An EMI-based approach for Structural Health Monitoring of a Space Reinforced Concrete Frame Structure

George M. Sapidis[1, 0000-0002-0240-5699], Maria C. Naoum[1, 0000-0002-2262-8267], Nikos A. Papadopoulos[1, 0009-0007-1183-4616], Maristella E. Voutetaki[2, 0000-0003-2420-9696], Constantin E. Chalioris[1, 0000-0001-8283-1382], Theodoros C. Rousakis[1, 0000-0002-6384-1451]
[1]Laboratory of Reinforced Concrete and Seismic Design of Structures, Civil Engineering Department, School of Engineering, Democritus University of Thrace – Xanthi 67100, Greece
[2]Structural Science and Technology Division, Architectural Engineering Department, School of Engineering, Democritus University of Thrace – Xanthi 67100, Greece
email: gsapidis@civil.duth.gr, mnaoum@civil.duth.gr, nikpapad@civil.duth.gr, mvouteta@arch.duth.gr, chaliori@civil.duth.gr, trousak@civil.duth.gr

ABSTRACT: The electro-mechanical impedance (EMI) method represents a promising approach to structural health monitoring (SHM), attributable to its ability to simultaneously employ piezoelectric transducers for both actuation and sensing purposes. As a result, an extensive volume of literature has surfaced recently, analyzing the efficacy of the EMI method in reinforced concrete (RC) structural elements subjected to quasi-static loading sequences. Nevertheless, the investigation into applying the EMI method in dynamic loading environments must be more robust within the current body of research. This study evaluates the effectiveness of the EMI method for SHM of a one-bay, one-story RC space frame structure under the influence of earthquake excitations. Therefore, a shaking table was used to excite the RC frame with progressively increased ground excitation, wherein piezoelectric patches are strategically embedded in meticulously chosen locations. The embedded PZT sensors facilitate promptly diagnosing earthquake-induced damage to the RC frame. The experimental outcomes reveal that the EMI method effectively and expeditiously identified damage formation within the RC frame.

KEY WORDS: Structural Health Monitoring (SHM), Electro-Mechanical Impedance (EMI), damage diagnosis, dynamic loading, Reinforced Concrete (RC) frame.

1 INTRODUCTION

In recent years, the secure extension of the service life of existing Reinforced Concrete (RC) structures has become critically significant due to the aging of a substantial portion of the European building stock, some of which have attained their original design life [1]. Therefore, Structural Health Monitoring (SHM) methods have emerged as an indispensable instrument for achieving this objective by evaluating their seismic performance and structural integrity [2]. Compared to conventional methods, such as visual inspection, SHM systems offer continuous inspection, enabling the detection of even slight internal damage initiation, by covering the 3D space of the structural mass in real-time rather than only after it becomes visibly apparent. These systems are permanently installed on the structure, allowing for ongoing monitoring without the need for manual inspections. Furthermore, the energy renovation of existing buildings increases the challenges associated with implementing conventional methods, given that the RC members are inaccessible due to the insulating materials. In contrast to traditional methods, the newly developed SHM techniques enable continuous monitoring and prompt damage identification. Consequently, these limitations have catalyzed SHM advancement in recent decades, during which several methodologies have emerged [3,4].

The electro-mechanical impedance (EMI) technique, recognized as one of the emerging methods in SHM, utilizes the coupling properties inherent in piezoelectric materials, notably lead zirconate titanate (PZT), to identify the deterioration of the assessed structure's mechanical properties. Furthermore, the damage within RC structures initially presents as distributed microcracks that localize to form significant visible cracks [5]. Additionally, a concentration of strain is observed within the material medium, accompanied by a decrease in the material stiffness matrix, before the emergence of visible cracks [6,7]. Consequently, the deterioration of the mechanical properties of the structure material is manifested in the EMI response of an affixed PZT transducer. Within the extensive body of literature, two primary methodologies are identified for the application of PZT transducers in RC structures: the utilization of externally bonded patches [8,9] or their integration as smart aggregates within the RC structures [10,11]. According to Naoum et al., embedded PZT sensors, like smart aggregates, exhibit increased sensitivity to damage formation and stress fields of the host structure compared to externally bonded PZT patches [12].

Consequently, many research papers have been published investigating the efficacy of EMI-based monitoring of RC elements. The EMI method has been widely utilized in studies for prompt load-induced damage detection of RC and FRC beams. Furthermore, research initiatives have examined the viability of the EMI method for SHM of full-scale subassemblies of RC structures, including RC beams [13–16] and RC joints [17,18] under quasi-static loading, yielding promising outcomes. In addition, research implements machine learning techniques to increase the robustness of the EMI method in high-complexity scenarios, such as retrofitted RC members [19–22]. Nevertheless, prior research has predominantly concentrated on damage identification utilizing quasi-static loading conditions, and research regarding the SHM of RC structures under dynamic loads remains notably limited.

As aforementioned, SHM methods, particularly the EMI method, have been widely investigated in RC subassemblies. However, there has been a dearth of research concerning entire RC structures. Kaur et al. examine the effectiveness of the EMI method in evaluating the pre-stressing force losses in the Sarey

DOI: 10.3217/978-3-99161-057-1-172

Kale Khan Bridge in New Delhi [23]. Moreover, Liao and Chiu investigate a PZT-based active sensing system designed for SHM of a one-bay, two-story RC space frame structure subjected to seismic loads [24]. A distributed array of PZT SAs was utilized, with specific units designated as actuators while others function as sensors. This approach contrasts with the EMI method, which employs the smart aggregates in dual roles as both actuators and sensors concurrently. Consequently, the EMI method requires fewer PZT transducers to monitor the same structure.

In this work, PZT transducers were embedded as smart aggregates in a one-bay, one-story RC space frame structure. Specifically, three PZT sensors were strategically positioned along the height of the RC columns for EMI-based SHM. Subsequently, the RC space frame underwent testing on a shaking table, with the Peak Ground Acceleration (PGA) level incrementally increased. To attain this incremental loading, a spectrogram of the substantial ground motion that significantly impacted Thessaloniki in 1978 was meticulously altered and determined the dynamic motion of the shaking table. Between the seismic sequences, the EMI responses of the PZT transducers were captured via a novel autonomous monitoring device. The obtained EMI signatures were utilized to expedite the identification of damage within the RC columns during the shake table test. The results underscore the viability and sensitivity of the EMI-based methodology for SHM of RC space frame structures subjected to seismic excitations.

2 ELECTROMECHANICAL IMPEDANCE METHOD

As previously indicated, the EMI method capitalizes on the unique characteristics of piezoelectric materials to generate surface electric charges when these materials are subjected to mechanical stress and experience mechanical deformation in response to an electric field [25,26]. Consequently, the reduction in mechanical impedance, associated with the formation of damage in RC members, significantly impacts the electrical impedance of a mounted piezoelectric transducer under harmonic excitation [27]. Furthermore, the EMI signatures of the attached piezoelectric transducers are frequently measured within a predefined frequency band. Any alteration in the EMI signature of each piezoelectric transducer signifies the development of structural damage in its vicinity. Therefore, numerous studies examine the interaction between an attached PZT transducer and the host structure, as exemplified in the work of Liang et al., who model this interaction [28].

In this study, a custom impedance analyzer excites the PZT transducers within a wide frequency range while simultaneously capturing the corresponding signals. Expressly, the EMI signature's frequency range was set between 10 and 250 kHz, with a resolution of 1 kHz. Initially, a set of measurements was taken before any seismic excitation to document the signatures of the PZTs in the healthy condition of the RC space frame structure. Subsequently, the EMI response of the PZT patches was recorded subsequent to the conclusion of each seismic excitation, while the specimen remained at rest. Then, each alteration of the EMI signature indicates the formation of damage in the monitoring area of each PZT sensor.

The interaction between the monitored structure and the PZT transducer significantly influences the EMI signature of the PZT. Consequently, the mechanical properties, including mass, damping, and Young's modulus, are reflected in the EMI signature of PZT due to these interactions. According to Bhalla and Soh, the interaction between the PZT transducer and the RC structure is depicted as an impedance signature that consists of resistance (the real component) and reactance (the imaginary component), as specified in Equation (1) for the complex impedance, Z(ω), of the affixed PZT transducer [29].

$$Z(\omega) = \frac{h}{2L^2\omega j}\left[\bar{\varepsilon}_{33}^{T} - d_{31}^2\bar{Y}^{E} + \left(\frac{Z_a}{Z_s+Z_a}\right)d_{31}^2\bar{Y}^{E}\left(\frac{\tan kL}{kL}\right)\right]^{-1} \quad (1)$$

h	PZT Thickness	k	wave number
L	Half-length of the PZT	Z_a	Effective mechanical impedance
ω	Angular frequency	Z_s	Effective structural impedance
j	Imaginary unit	d_{31}	Piezoelectric strain coefficient
$\bar{\varepsilon}_{33}^{T}$	Complex electric permittivity	$\bar{Y}^{E}$	Complex Young's modulus of the elasticity

Consequently, as indicated by Equation (1), any alterations observed in the electrical impedance of the connected PZT transducer arise from variations in the mechanical impedance of the monitored area, given that the other components of Equation (1) remain unaltered. Thus, notable variations in the EMI response measurements suggest the possibility of structural degradation in the monitored structure.

Researchers usually employ statistical scalar indices to quantify the damage from the EMI responses of the smart aggregates. This study uses the widely utilized damage index, Root Mean Square Deviation (RMSD). The RMSD quantifies the variations between the output signals at the pristine condition and after each loading sequence, according to Equation (2).

$$RMSD = \sqrt{\frac{\sum_{i=1}^{N}\left(|V_p(f)|_D - |V_p(f)|_H\right)^2}{\sum_{i=1}^{N}\left(|V_p(f)|_H\right)^2}} \quad (2)$$

Where: $|V_p(f)|_H$ represents the absolute value of the voltage output signal extracted from the smart aggregate under the pristine condition of the RC structure, $|V_p(f)|_D$ denotes the absolute value of the corresponding voltage output signal measured from the same smart aggregate at damage level D, and *N* is the discrete number of measurements taken within the frequency band of 10-250 kHz.

3 EXPERIMENTAL PROGRAM

3.1 Materials and Specimen

This experimental investigation entails casting a one-bay, one-story RC space frame structure, with four RC columns, four beams, a slab, four cantilevers and four infill masonry walls, all designed in accordance with old code provisions (1970s), before the adoption of current Eurocodes 2 and 8 or the New Greek Seismic Code for Concrete Structures. Furthermore, the specimen was scaled at a ratio of 1:3 in accordance with the capacity of the laboratory's shake table,

DOI: 10.3217/978-3-99161-057-1-172

which possessed a maximum tested structure mass of 8 tons and a maximum overturning moment of 8 ton·m. Therefore, the mass of the specimens was adjusted to 4.3 tonnes, which is less than the maximum bearing capacity of the shake table. The clear span of the specimen's beam measured 1.24 meters, and the clear height of the specimen's columns was 1.0 meters. The concrete utilized in this study was of a C20/25 grade, and the reinforcement employed was referenced as B500C for the slab and foundation and for the longitudinal reinforcement of the columns and S220 for the column stirrup. The column cross-section was set to 13×13 centimeters, and the reinforcement of the specimen was four longitudinal reinforcement bars, each measuring 8 millimeters in diameter, strategically positioned at each corner. Additionally, a closed smooth steel stirrup measuring 5,5 millimeters in diameter was placed every 6 centimeters to serve as transverse reinforcement. A reinforced concrete (RC) slab, which incorporates four balconies and four hidden beams, was constructed with a thickness of 20 centimeters on top of the columns. This heavily reinforced slab was utilized to drive the potential damage in the RC columns and the brick infill panels as well as to allow for additional mass due to renovations involving greenery (with special reference to Thessaloniki metropolitan area). Although the occurrence of damage in vertical structural components is undesirable under current seismic regulations, it is prevalent in existing buildings constructed under older standards (strong slab or beams and weak columns). Figure 1 illustrates the specimen positioned on the shake table in the pristine condition.

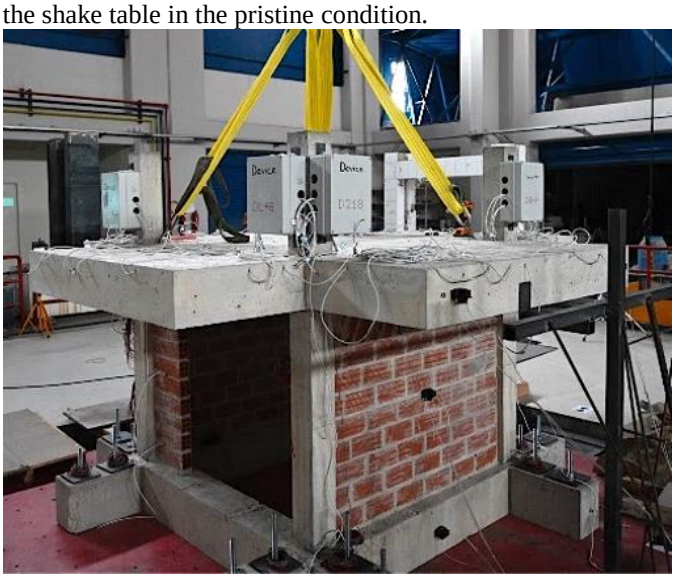

Figure 1. RC frame test setup.

3.2 Adopted SHM Scheme

As mentioned above, this study investigates a PZT-enabled EMI-based SHM approach for the SHM of a one-bay, one-story RC concrete structure. Thus, several PZT transducers were embedded as smart aggregates in the RC frame specimen. The fabrication of smart aggregates involves several stages. Initially, two lead wires were welded to the two poles of the PZT patch, and the functionality of the sensors was duly verified before further action steps. Subsequently, the PZT transducers were coated with a waterproof layer of epoxy resin, as illustrated in Figure 2. Then, the smart aggregates were positioned in meticulously selected locations of the RC specimen prior to the pouring of concrete. Although various PZT sensors were employed to monitor different aspects of the specimen's structural integrity, this study focuses on the prompt diagnosis of the formation of bending cracks in the critical regions of the columns. Therefore, two piezoelectric sensors were placed at various heights along the RC columns. The PZT Up and PZT Down were positioned within the critical region, where bending cracks were expected to develop, of the RC columns for the prompt detection of bending-associated crack formation, as depicted in Figure 2. As mentioned earlier, the EMI response of each PZT was recorded using portable EMI-based monitoring devices capable of capturing the EMI response of PZT transducers within the frequency spectrum of 10-250 kHz.

Figure 2. Ready to implement Smart Aggregate.

3.3 Shake Table Test Setup

The shake table tests were conducted at the laboratory of Reinforced Concrete and Seismic Design of Structures of Democritus University of Thrace, located in Xanthi, Greece. The shake table has dimensions of 3.4 m by 3.4 m and a maximum velocity of 1.2 m/sec. Furthermore, it possesses a maximum uniaxial acceleration capacity of 1.6g for a payload mass of eight tons and 2.9g for a payload mass of four tons. The maximum displacement capacity of the shaking table was 23 centimeters, and the range of response frequencies extended from 1.0 to 50.0 Hertz. Additionally, a dynamic capability data acquisition system acquired the data of twelve accelerometers, eight-string potentiometers, and 20 strain gauges. Three out of the 12 accelerometers were used to measure the out-of-plane acceleration of the infills. Four-string potentiometers were used to calculate the story drift of the RC structure, while the

DOI: 10.3217/978-3-99161-057-1-172

remaining devices were used to evaluate the deformation associated with the in-plane response of the infills. Furthermore, appropriate markers for vision-based SHM were strategically positioned on the surfaces of the specimens and employed to extract the displacement field from videos captured by two cameras positioned perpendicularly.

The dynamic loading involved the gradual increment of PGA levels up to 1,1g peak acceleration, based on the employed earthquake component from Thessaloniki in the north–south direction (peak acceleration of 0.14g with main excitation frequencies ranging from 2 Hz to 10 Hz and minor excitation frequencies beyond 26 Hz). The seismic event occurred on 20 June 1978 at 20:03:21 in the epicenter 30 kilometers east of Thessaloniki, revealing the susceptibility of urban centers to such natural disasters. According to Theodulidis et al., 4000 buildings experienced serious, 13000 moderate, and 49000 minor damage [30]. The north–south component of the strong ground motion record at the Thessaloniki-City Hotel station, situated 29 kilometers from the epicenter, offered the ground excitation time history utilized during the dynamic tests, as illustrated in Figure 3. Subsequently, this sequence has been meticulously adjusted to stimulate the specimen with peak accelerations of up to 0.1g, 0.2g, 0.5g, 0.8g, and 1.1g, following a dynamic pushover approach. The ultimate level of the first phase of testing of the as-built structure (presented herein) was characteristic of a structure with RC members at Serviceability Limit States (SLS), where no yielding of steel rebars occurred and brick infills with damage initiation but no collapse. Thereafter, the EMI response of all the PZT sensors was recorded following each excitation.

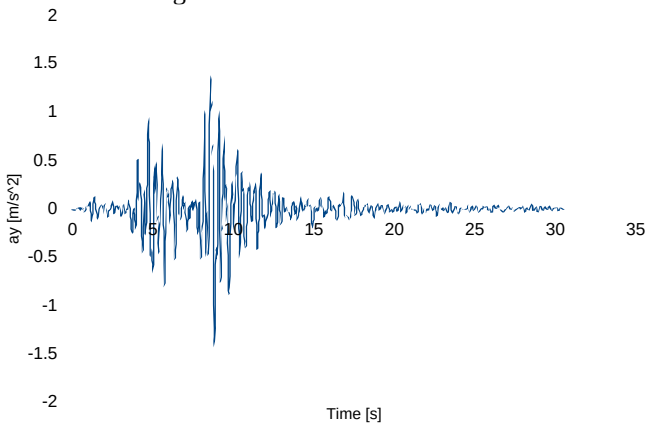

Figure 3. Ground acceleration time history.

4 TEST RESULTS

4.1 Cracking patterns of RC columns

This sub-section addresses the earthquake-induced damage of the specimen and its observed cracking pattern. The specimen underwent five progressively enhancing sequences of ground excitation. After the third test run, which corresponds to a peak acceleration of 0.5g, some slight surface cracks were observed in the lower region of the RC columns. Therefore, the EMI response captured after the first and second test runs was designated as pre-crack, in conjunction with the EMI response measured under pristine structural conditions. Conversely, the EMI response obtained following the third test run, and the formation of the first cracks, was classified as post-crack. The cracks were further propagated during the subsequent loading sequences. Figure 4 illustrates the damage condition of the RC \column Y1 after all the loading sequences. A bending crack was formed in the lower region of the column, in proximity to the PZT Y1B. Despite the crack propagating through the entirety of the column's cross-section, the measured width of the crack along with the recorded reinforcement strain suggests that the damage sustained was not severe.

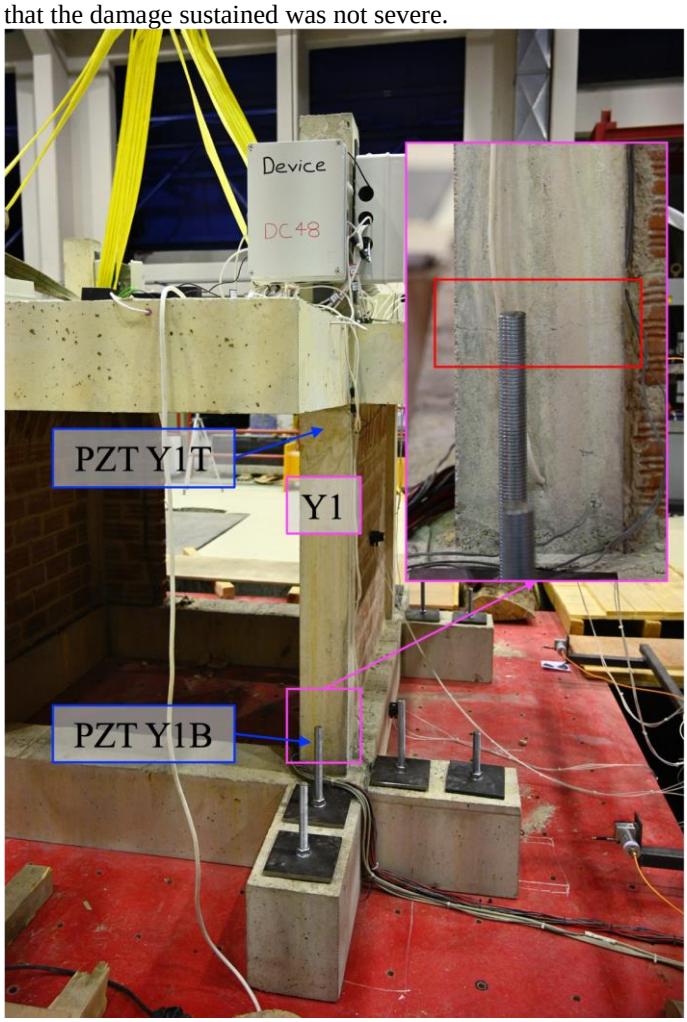

Figure 4. Damage state of RC column Y1

Furthermore, Figure 5 depicts the damage condition of the reinforced concrete column Y2 following the completion of the final loading sequences. In contrast to column Y1, column Y2 was in contact with infills in the biaxial direction. Notwithstanding the fact that the in-plane infill did not encompass the entire span, it nonetheless merely enhanced the load-bearing capacity and the overall stiffness of the specimen. A minor bending crack has developed in the lower region of column Y2, which was sustained in a portion of the column's cross-section, in contrast to the bending crack of column Y1. This may have been attributed to the beneficial contribution of the brick infill. Similarly to column Y1, the crack width and the steel reinforcement strain indicate that the damage sustained was not severe. Therefore, although cracks developed in the RC columns and the brick infill, the structural condition of the space RC frame specimen is categorized within the SLS, as determined by the experimental design for the initial testing phase, as previously noted.

DOI: 10.3217/978-3-99161-057-1-172

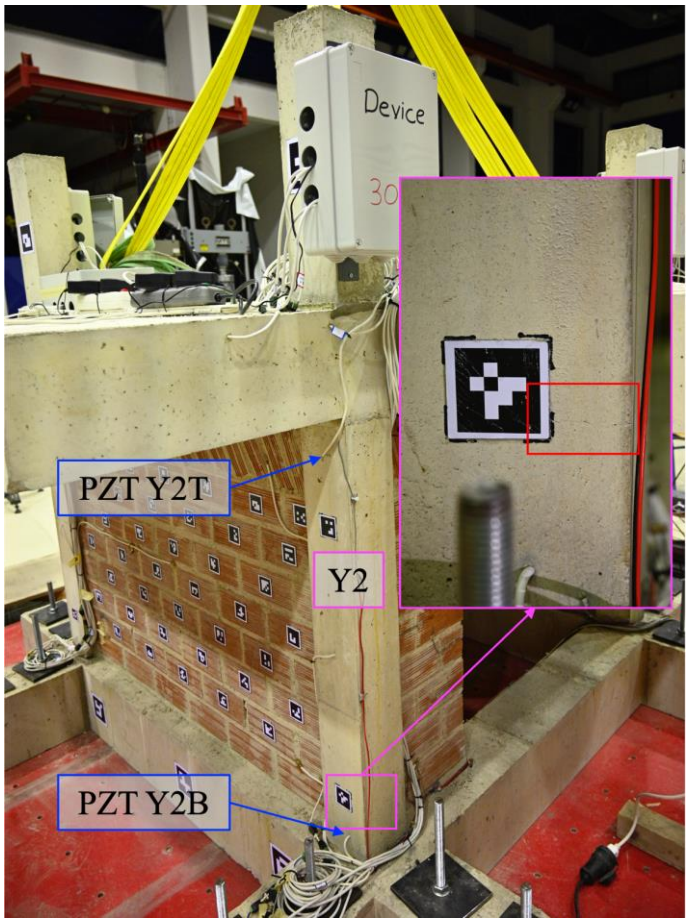

Figure 5. Damage state of RC column Y2

4.2 The EMI response of smart aggregates

This sub-section presents the EMI response of each PZT transducer in terms of Vp—excitation frequency, as captured with the RC specimen at rest. The EMI responses were measured across a broad frequency spectrum from 10 to 250 kHz. Figure 6 illustrates the EMI response of PZT Y1B, which was placed in the lower region of column Y1. The EMI response of PZT Y1B demonstrated a leftward shift subsequent to the formation of a bending crack in its vicinity. Furthermore, the EMI response does not demonstrate any additional alterations, which aligns with the observed cracking pattern, where the crack width remains constant. Thus, the proposed SHM scheme promptly identifies the formation of the bending crack in the lower region of the column through the alterations of the PZT Y1B EMI responses.

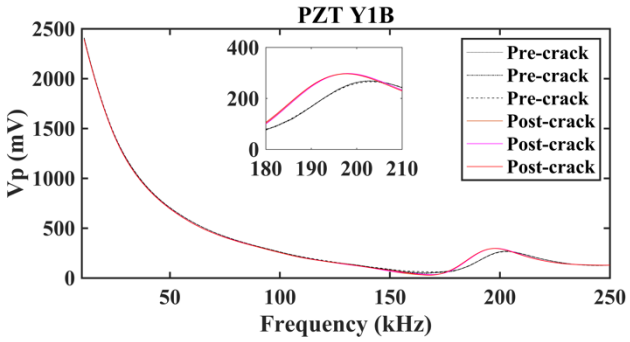

Figure 6. The EMI response of PZT Y1B

Figure 7 shows the EMI response of PZT Y1T, which was placed in the upper region of column Y1. In contrast to the smart aggregate PZT Y1B, the EMI response of PZT Y1T does not vary significantly, as verified by the RMSD values in the following subsection. These findings are consistent with the column's observed crack patterns, wherein the fissure developed in its lower region, as depicted in Figure 4.

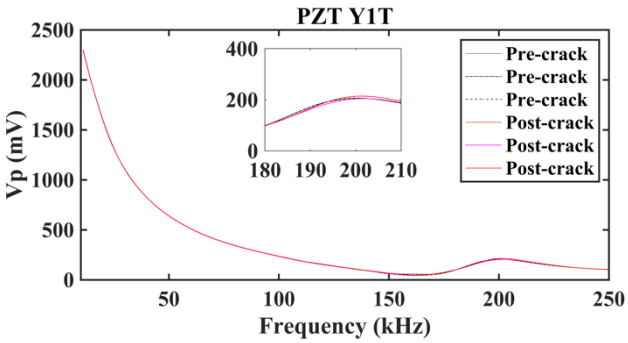

Figure 7. The EMI response of PZT Y1T

Figure 8 depicts the EMI response of PZT Y2B, which was placed in the lower region of column Y2. The EMI response exhibits a subtle peak shift resulting from the development of a bending crack in proximity to the smart aggregate. This is in line with the observed crack patterns of column Y2, as illustrated in Figure 5.

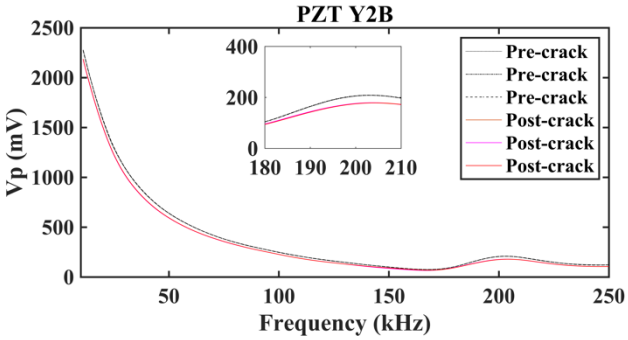

Figure 8. The EMI response of PZT Y2B

Figure 9 illustrates the EMI response of PZT Y2T, which was placed in the upper region of column Y2. No observable alterations in the EMI response of the smart aggregate PZT Y2T, which may be attributed to the distance of the formed bending crack.

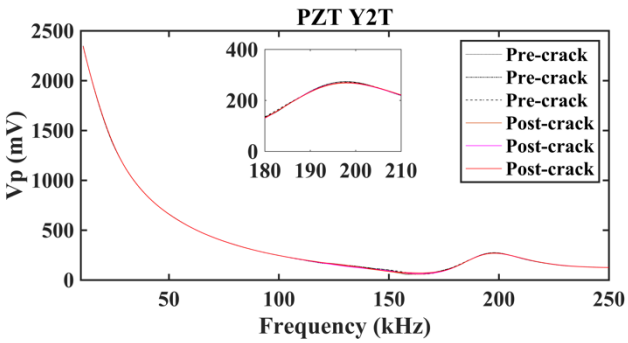

Figure 9. The EMI response of PZT Y2T

4.3 The RMSD

As previously mentioned, the RMSD damage index utilized to quantify the variations in the EMI responses of PZTs in this

DOI: 10.3217/978-3-99161-057-1-172

study. Figure 10 illustrates the RMSD values of the smart aggregates situated in the upper and lower sections of Column 1. Evidently, the development of a bending crack in column Y1 initiates a significant increase in the RMSD values of PZT Y1B, escalating from 0.5% to 3.2%. On the contrary, the RMSD values of PZT Y1T remain around 0.5 throughout the seismic sequences.

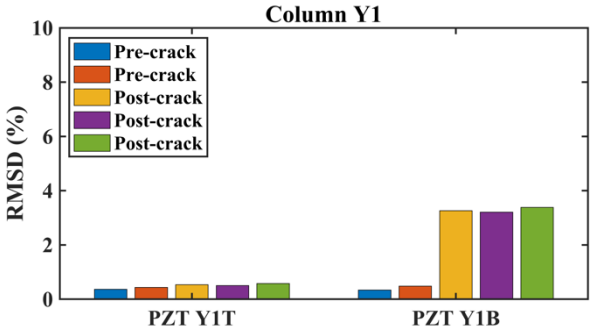

Figure 10. RMSD damage index values pertaining to the smart aggregates in Column Y1

Additionally, Figure 11 depicts the RMSD values of the corresponding smart aggregates of column 2. Similarly, the RMSD values of PZT Y2B demonstrate a significant increase, rising from 0.4% to 6%. Thus, PZT Y2B has effectively identified the development of a bending crack in the lower section of column Y2. Furthermore, RMSD values of PZT Y2T fluctuated between 0.5 and 0.7 during the seismic sequences. Consequently, the SHM scheme indicates that damage has occurred in the lower region of both columns, which aligns with the observations.

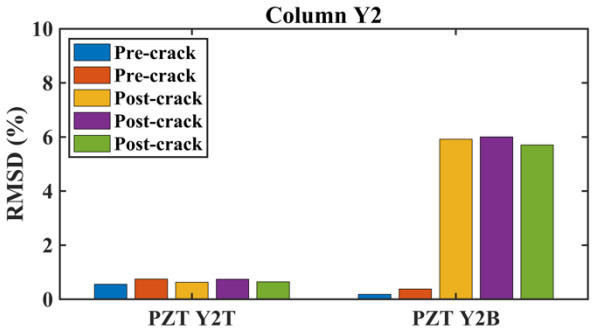

Figure 11. RMSD damage index values pertaining to the smart aggregates in Column Y2

5 CONCLUSIONS

This study addresses the feasibility of the EMI method for SHM of a one-bay, one-floor space RC frame structure subjected to earthquake excitations. The specimen was subjected to various percentages of PGA of a strong seismic event, resulting in bending cracks in the lower regions of the specimen's RC columns. The structural integrity has been classified into two distinct categories, referred to as pre-crack and post-crack. The EMI method effectively identified the formation of cracks through the variation induced in the EMI responses of the smart aggregates, indicating its feasibility for the SHM of RC structures. Additionally, it successfully localized these cracks within the lower regions of the specimen's columns. SHM was successful even though this study was limited to minor damage conditions, relatively close to SLS of RC structures. Such RC damages are hard to detect as the residual drift of the structure is negligible. Subsequent research should further explore the efficacy of the EMI method under conditions approaching the near-collapse damage condition of RC structures as well as the effects due to additional mass after innovative renovations.

ACKNOWLEDGMENTS

The research project is implemented in the framework of H.F.R.I call “Basic research Financing (Horizontal support of all Sciences)” under the National Recovery and Resilience Plan “Greece 2.0” funded by the European Union—NextGenerationEU (H.F.R.I. Project Number: 015376). https://greenergy.civil.duth.gr/

REFERENCES

[1] Palermo, V.; Maio, R.; Sousa, M.; Tsionis, G. Framework for resilience analysis of EU buildings. [Internet]. LU: Publications Office European Commission. Joint Research Centre.; 2017 [cited 2025 Mar 23]. Available from: https://data.europa.eu/doi/10.2760/923762

[2] Kassem MM, Beddu S, Ooi JH, Tan CG, Mohamad El-Maissi A, Mohamed Nazri F. Assessment of Seismic Building Vulnerability Using Rapid Visual Screening Method through Web-Based Application for Malaysia. Buildings. 2021 Oct 18;11(10):485.

[3] Farrar CR, Jauregui DA. Comparative study of damage identification algorithms applied to a bridge: I. Experiment. Smart Mater Struct. 1998 Oct 1;7(5):704–19.

[4] Nagarajaiah, Satish, Erazo, Kalil. Structural monitoring and identification of civil infrastructure in the United States. Structural Monitoring and Maintenance. 2016 Nov 25;3[1]:51–69.

[5] Narayanan A, Subramaniam KVL. Sensing of damage and substrate stress in concrete using electro-mechanical impedance measurements of bonded PZT patches. Smart Mater Struct. 2016 Sep 1;25(9):095011.

[6] Surendra P. Shah and Sushil Chandra. Critical Stress, Volume Change, and Microcracking of Concrete. ACI Journal Proceedings. 1968 Jan 9;65(9).

[7] V. S. Gopalaratnam and Surendra P. Shah. Softening Response of Plain Concrete in Direct Tension. ACI Journal Proceedings. 1985 Jan 5;82(3).

[8] Sapidis G, Naoum M, Papadopoulos N, Voutetaki M. Flexural Damage Evaluation in Fiber Reinforced Concrete Beams Using a PZT-Based Health Monitoring System. In: Jędrzejewska A, Kanavaris F, Azenha M, Benboudjema F, Schlicke D, editors. International RILEM Conference on Synergising Expertise towards Sustainability and Robustness of Cement-based Materials and Concrete Structures [Internet]. Cham: Springer Nature Switzerland; 2023 [cited 2023 Jul 3]. p. 957–68. (RILEM Bookseries; vol. 43). Available from: https://link.springer.com/10.1007/978-3-031-33211-1_86

[9] Sapidis GM, Naoum MC, Papadopoulos NA. Electromechanical Impedance-Based Compressive Load-Induced Damage Identification of Fiber-Reinforced Concrete. Infrastructures. 2025 Mar 10;10(3):60.

[10] Ai D, Li H, Zhu H. Flexure-critical stress and damage identification in RC beam structure using embedded piezoelectric transducers: 2D modelling and experimental investigations. Construction and Building Materials. 2023 Dec;409:134017.

[11] Papadopoulos NA, Naoum MC, Sapidis GM, Chalioris CE. Resilient and Sustainable Structures through EMI-Based SHM Evaluation of an Innovative C-FRP Rope Strengthening Technique. Applied Mechanics. 2024 Jun 21;5(3):405–19.

[12] Naoum MC, Sapidis GM, Papadopoulos NA, Voutetaki ME. An Electromechanical Impedance-Based Application of Realtime Monitoring for the Load-Induced Flexural Stress and Damage in Fiber-Reinforced Concrete. Fibers. 2023 Apr 11;11(4):34.

[13] Ai D, Luo H, Wang C, Zhu H. Monitoring of the load-induced RC beam structural tension/compression stress and damage using piezoelectric transducers. Engineering Structures. 2018 Jan;154:38–51.

[14] Naoum MC, Papadopoulos NA, Sapidis GM, Chalioris CE. Advanced Structural Monitoring Technologies in Assessing the Performance of Retrofitted Reinforced Concrete Elements. Applied Sciences. 2024 Oct 12;14(20):9282.

DOI: 10.3217/978-3-99161-057-1-172

[15] Angeli GM, Naoum MC, Papadopoulos NA, Kosmidou PMK, Sapidis GM, Karayannis CG, et al. Advanced Structural Technologies Implementation in Designing and Constructing RC Elements with C-FRP Bars, Protected Through SHM Assessment. Fibers. 2024 Dec 5;12(12):108.
[16] Papadopoulos NA, Naoum MC, Sapidis GM, Chalioris CE. Cracking and Fiber Debonding Identification of Concrete Deep Beams Reinforced with C-FRP Ropes against Shear Using a Real-Time Monitoring System. Polymers. 2023 Jan 17;15(3):473.
[17] Divsholi BS, Yang YW, Bing L. Monitoring Beam-Column Joint in Concrete Structures Using Piezo-Impedance Sensors. AMR. 2009 Aug;79–82:59–62.
[18] Naoum M, Sapidis G, Papadopoulos N, Golias E, Chalioris C. Structural Health Monitoring of Reinforced Concrete Beam-Column Joints Using Piezoelectric Transducers. In: Jędrzejewska A, Kanavaris F, Azenha M, Benboudjema F, Schlicke D, editors. International RILEM Conference on Synergising Expertise towards Sustainability and Robustness of Cement-based Materials and Concrete Structures [Internet]. Cham: Springer Nature Switzerland; 2023 [cited 2023 Jul 6]. p. 945–56. (RILEM Bookseries; vol. 43). Available from: https://link.springer.com/10.1007/978-3-031-33211-1_85
[19] Perera R, Torres L, Ruiz A, Barris C, Baena M. An EMI-Based Clustering for Structural Health Monitoring of NSM FRP Strengthening Systems. Sensors. 2019 Aug 31;19(17):3775.
[20] Ai D, Mo F, Han Y, Wen J. Automated identification of compressive stress and damage in concrete specimen using convolutional neural network learned electromechanical admittance. Engineering Structures. 2022 May;259:114176.
[21] Sapidis GM, Kansizoglou I, Naoum MC, Papadopoulos NA, Chalioris CE. A Deep Learning Approach for Autonomous Compression Damage Identification in Fiber-Reinforced Concrete Using Piezoelectric Lead Zirconate Titanate Transducers. Sensors. 2024 Jan 9;24(2):386.
[22] Sapidis GM, Naoum MC, Papadopoulos NA, Golias E, Karayannis CG, Chalioris CE. A Novel Approach to Monitoring the Performance of Carbon-Fiber-Reinforced Polymer Retrofitting in Reinforced Concrete Beam–Column Joints. Applied Sciences. 2024 Oct 10;14(20):9173.
[23] Kaur N, Goyal S, Anand K, Sahu GK. A cost-effective approach for assessment of pre-stressing force in bridges using piezoelectric transducers. Measurement. 2021 Jan;168:108324.
[24] Liao WI, Chiu CK. Seismic Health Monitoring of a Space Reinforced Concrete Frame Structure Using Piezoceramic-Based Sensors. J Aerosp Eng. 2019 May;32(3):04019015.
[25] Ha SK, Keilers C, Chang FK. Finite element analysis of composite structures containing distributed piezoceramic sensors and actuators. AIAA Journal. 1992 Mar;30(3):772–80.
[26] Ikeda T, Ikeda T. Fundamentals of piezoelectricity. 1. issued in paperback with corr. Oxford: Oxford University Press; 1996. 263 p. (Oxford science publications).
[27] Liang C, Sun F, Rogers CA. Electro-mechanical impedance modeling of active material systems. Smart Mater Struct. 1996 Apr 1;5(2):171–86.
[28] Liang C, Sun FP, Rogers CA. An Impedance Method for Dynamic Analysis of Active Material Systems. Journal of Intelligent Material Systems and Structures. 1997 Apr;8(4):323–34.
[29] Bhalla S, Soh CK. Electromechanical Impedance Modeling for Adhesively Bonded Piezo-Transducers. Journal of Intelligent Material Systems and Structures. 2004;15(12):955-972.
[30] Theodulidis N, Roumelioti Z, Panou A, Savvaidis A, Kiratzi A, Grigoriadis V, et al. Retrospective Prediction of Macroseismic Intensities Using Strong Ground Motion Simulation: The Case of the 1978 Thessaloniki (Greece) Earthquake (M6.5). Bull Earthquake Eng. 2006 May;4(2):101–30.